Effect of flax fiber orientation on machining behavior and surface finish of natural fiber reinforced polymer composites

Faissal Chegdani[a,c,*], Behrouz Takabi[b], Mohamed El Mansori[a,d], Bruce L. Tai[b], Satish T.S. Bukkapatnam[c,d]

[a] Arts et Métiers Institute of Technology, MSMP, HESAM Université, F-51006, Châlons-en-Champagne, France
[b] Texas A&M University, Department of Mechanical Engineering, 3123 TAMU, College Station, TX, 77843, USA
[c] Texas A&M University, Department of Industrial and Systems Engineering, 3131 TAMU, College Station, TX, 77843, USA
[d] Texas A&M Engineering Experiment Station, Institute for Manufacturing Systems, College Station, TX 77843, USA

Keywords:
Natural fiber composites
Machining
Fiber orientation
Mechanical testing
Cutting tribology
Merchant model

A B S T R A C T

Manufacturing processes of natural fiber reinforced polymer (NFRP) composites are becoming the interest of industrials and scientists because these eco-friendly materials are emerging in automotive and aerospace industries. In this context, machining processes of NFRP composites present significant issues related to the complex structure of natural fibers that need thorough tribological studies. This paper aims to explore the effect of natural fiber orientation on the machinability of NFRP composites using Merchant model in order to separate the shearing energy from the friction energy. Orthogonal cutting process is conducted on unidirectional flax fibers reinforced polypropylene composites by changing the fiber orientation from 0° to 90° with respect to the cutting direction. Iosipescu shear tests are also performed to determine the mechanical shear behavior in function of the fiber orientation. Results show the applicability of Merchant model on the machining analysis of NFRP composites by verifying the main model assumptions. The fiber orientation affects significantly the shearing and the friction energies that control the cutting behavior and the chip formation of the NFRP composite. The resulted machined surfaces are hence intimately related to the natural fiber orientation.

1. Introduction

The use of natural fibers, especially plant fibers, as reinforcement for composite materials has become increasingly common in many industrial sectors as a substitute for synthetic glass fibers [1–5] in order to reduce the environmental impacts and thus contribute to a circular economy and sustainable development [6–8]. However, manufacturing processes of these eco-friendly materials encounter technical and technological barriers [9]. In particular, machining processes of natural fiber composites need deep investigations to optimize the machinability in terms of surface damages, surface topography, and tool wear [10–12].

The orientation of fibers within the composites is revealed among the most significant parameters that affect the machinability of synthetic composites [13–18]. Indeed, the cutting forces are influenced by the orientation of fibers regarding the cutting direction [13,16]. Depending on the fiber orientation, the chip is formed ahead of the cutting tool edge by the shearing of the matrix along the fiber/matrix interface [15]. The chip size decreases with an increase in the fiber orientation up to 45° from the cutting direction, while discontinuous and powder-like chips are produced after reaching 45° from the cutting direction [17].

Machining of natural fiber reinforced polymer (NFRP) composites has been investigated experimentally by testing the effect of process parameters (cutting speed, feed, and tool geometry) on the machined surface and the composite delamination using the conventional machining processes such as drilling and milling [19–24]. All these studies show that the cutting behavior of natural fiber composites is different from that of synthetic fiber composites, which is due to the complex cellulosic structure of natural fibers [25]. This finding was confirmed by the fundamental process of orthogonal cutting to show that the chip formation of natural fiber composites differs from that of synthetic fiber composites [26]. However, the effect of fiber orientation on the machinability of natural fiber composites has not yet been investigated in depth although this parameter could have a noticeable impact on the cutting behavior of natural fibers because of their high structural anisotropy [25].

The machining model of Merchant was developed to investigate the

* Corresponding author at: Arts et Metiers Institute of Technology, MSMP, HESAM Université, F-51006, Châlons-en-Champagne, France.
E-mail address: faissal.chegdani@ensam.eu (F. Chegdani).

https://doi.org/10.1016/j.jmapro.2020.03.025

cutting mechanisms of metallic materials in the configuration of orthogonal cutting [27]. Merchant model has been applied to orthogonal cutting of PA66 polyamide (with and without glass fiber reinforcement) and similar results were obtained when comparing Merchant model outputs with experimental findings [28]. Merchant's approach was also applied to the cutting of carbon fiber reinforced epoxy composites by assuming that the shear plane angle is identical to the fiber orientation angle where failure occurs [15]. The shear angle (ϕ) was then substituted by the fiber orientation angle (θ) in the Merchant model.

In this paper, the applicability of Merchant model is investigated on the machining of natural fiber composites using unidirectional flax fiber reinforced polypropylene (UDF/PP). After the validation of the main model assumptions, the effect of fiber orientation on the machinability of natural fiber composites is hence analyzed using the Merchant model in order to study the shearing and the friction phenomena during the orthogonal cutting process.

2. Experimental procedure

2.1. NFRP composites based on flax fibers and polypropylene matrix

NFRP samples are composed of unidirectional flax fibers reinforced polypropylene (UDF/PP) composite. The UDF/PP workpieces shown in Fig. 1(a) are manufactured and supplied by "*Composites Evolution – UK*". The fiber volume fraction is 40 % and their unidirectionality is maintained by polyester weft fiber with low volume fraction (less than 5%) so they do not affect the present mechanical and machining investigations. Fig. 1(b) shows the random distribution of flax fibers inside the composite in addition to a high variability of fibers shape and diameter. Moreover, flax fibers are either separated into elementary fibers or grouped into bundles called technical fiber as shown in Fig. 1(b).

2.2. Mechanical testing of UDF/PP composites

UDF/PP specimens have first been mechanically tested using Iosipescu shear experiments [29,30] in order to investigate the effect of flax fiber orientation on the shear behavior as shown in Fig. 2. Shear strain is acquired with biaxial strain gages (Model CEA-06-125WT-350) and using a displacement velocity of 2 mm/min. The shear motion is ensured by embedding the sample on the left side and applying a normal force on the right side as shown in Fig. 2(b). Three fiber orientation (θ in Fig. 2(b)) are considered in this study (θ = 0°, θ = 45° and θ = 90°). Each shear test is repeated three times to get repeatable results.

2.3. Orthogonal cutting setup

The orthogonal cutting setup is composed of two linear actuators as shown in Fig. 3. Their motion is maintained by high-torque smart motors (L70, Moog Animatics, Milpitas, CA). The rotation is converted to a linear motion through a ball screw. A polycrystalline diamond (PCD) cutting insert (model Sandvik TCMW16T304FLP-CD10) is attached to one linear actuator (M1) through a customized tool holder. The NFRP workpiece is attached to the other linear actuator (M2) through a mechanical clamping system. A Kistler dynamometer (model 9272) is mounted between the slider (S2) and the clamping system to acquire the cutting forces. The linear actuator M1 provides the cutting speed, while the linear actuator M2 controls the cutting depth. High-speed camera (Phantom Miro Lab310, Vision Research Inc.,Wayne, NJ) is used to capture the in-situ chip formation. The high-speed camera is set with 640 × 480 resolution, 1000 fps, 1000 µs exposure time, and appropriate lightening to capture the best view of the in-situ chip morphology.

Table 1 summarizes the cutting conditions considered for this investigation. Each cutting configuration is tested three times to assure the repeatability. Thus, the final outputs from the orthogonal cutting experiments are presented as the mean value of these three repeated tests. Measurement errors are considered as the average of the absolute deviations of data repeatability tests from their mean. All the considered workpieces have the geometric dimensions of 20 × 15 × 4 mm.

The cutting edge radius (r_ε) of the PCD insert is measured with an Atomic Force Microscope (AFM) instrument (model Dimension Edge™ - Bruker) using Tapping mode in order to evaluate the tool sharpness. Fig. 4 shows the surface topography measurements of the cutting edge that allows the calculation of the cutting edge radius by extracting the 2D profile sections (Fig. 4(c)) at different locations from the 3D surface topography of Fig. 4(b). The resulting cutting edge radius is founded to be $r_\varepsilon = 3.23^{\pm 0.4}$ µm.

2.4. Surface finish characterization

Machined surfaces states are qualitatively analyzed by scanning electron microscope SEM Zeiss EVO/MA10 at low vacuum mode (40 Pa of chamber pressure). SEM images are taken at different locations on the machined surfaces. Representative surfaces morphology as induced by orthogonal cutting is presented in this paper. Removed chip profiles are also investigated using another SEM device JSM –5510LV at low vacuum mode (10 Pa of chamber pressure) in order to calculate the removed chip thickness. Furthermore, the machined surfaces topography is quantitatively evaluated by the optical interferometer Model ZYGO/14-21-75092 using a magnification of ×10. Topographic images are taken in five different locations of each machined surface to determine the arithmetical mean height of the surface Sa following the ISO 25178 standard.

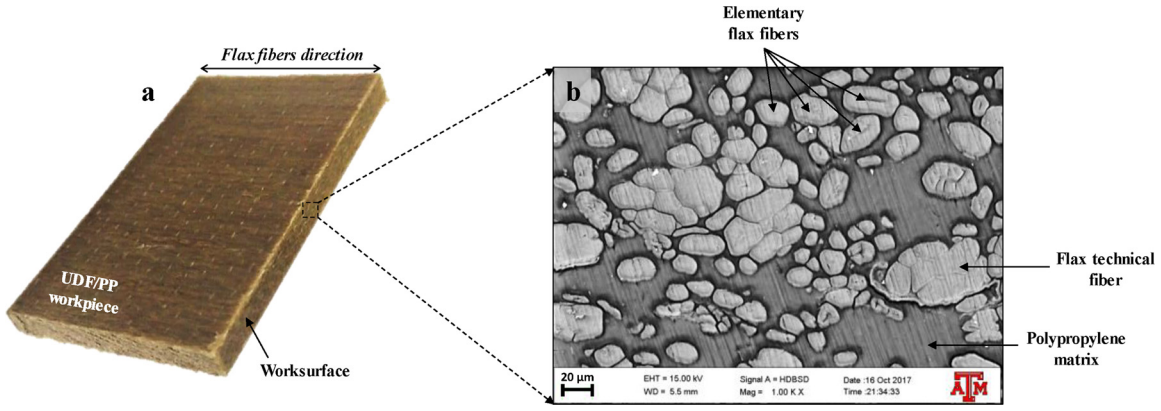

Fig. 1. a) photograph of UDF/PP workpiece with 90° of fiber orientation. b) SEM image of the UDF/PP worksurface in the case of 90° of fiber orientation showing the fibers cross-sections.

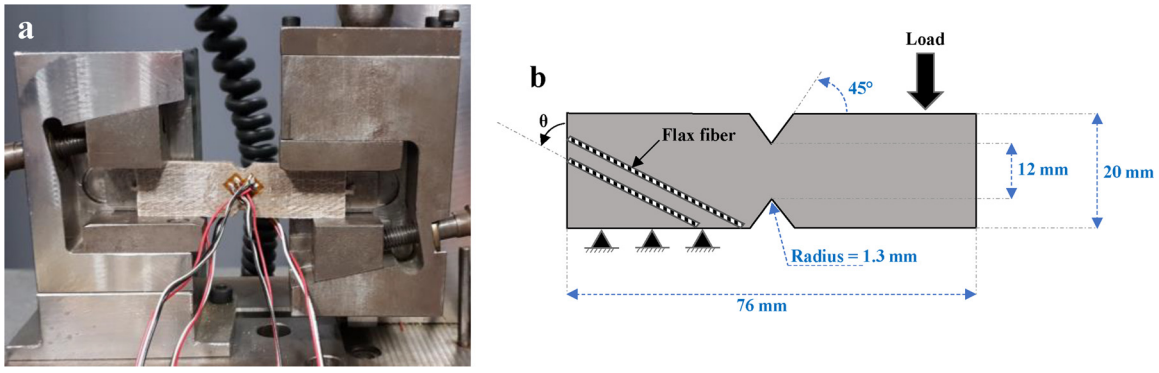

Fig. 2. a) Iosipescu shearing device. b) Schematic illustration of the Iosipescu shearing specimen showing the sample dimensions and the loading conditions.

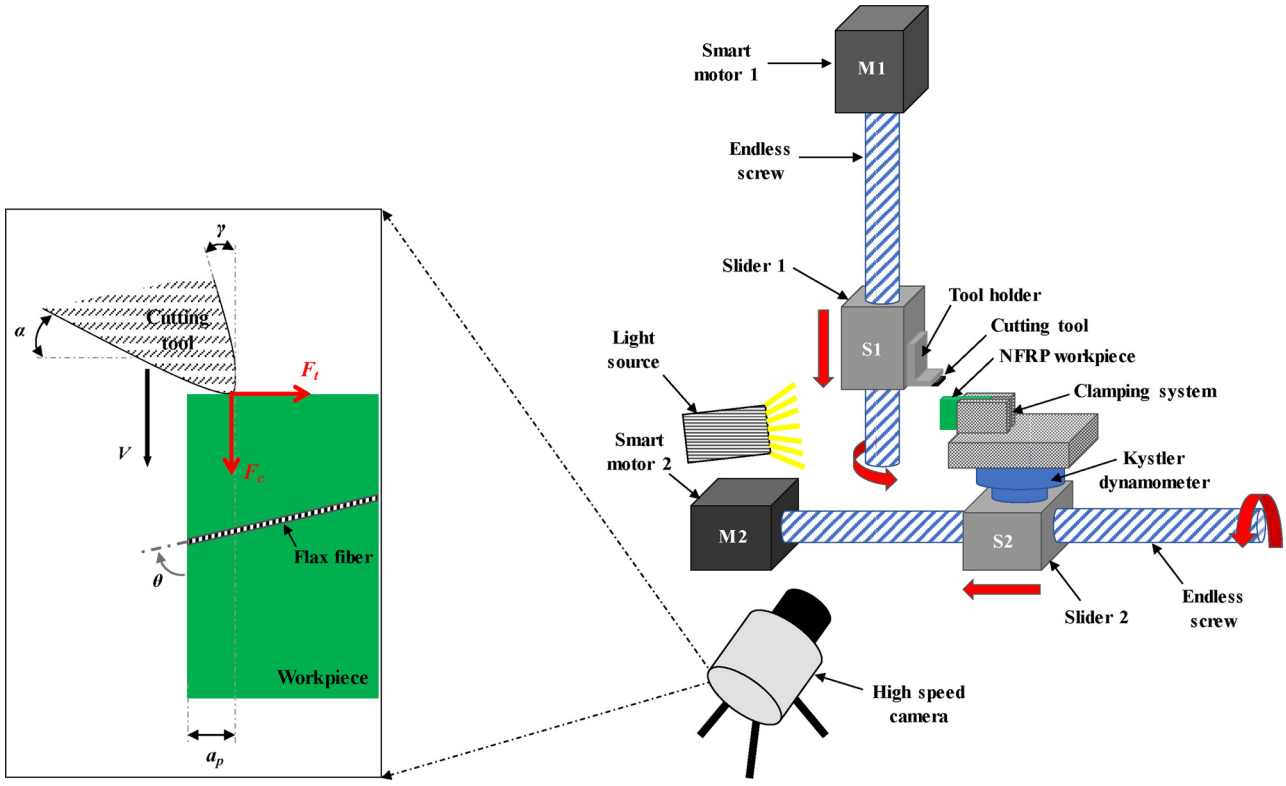

Fig. 3. Schematic of the experimental setup for orthogonal cutting tests.

Table 1
Cutting conditions considered for orthogonal cutting tests.

Flax fiber orientation (θ)	Cutting speed V(m/min)	Depth of cut a_p (μm)
	2	100
	4	
0°	6	
45°	8	
90°	10	
	12	

3. Results and discussion

3.1. Fiber orientation effect on the shear behavior of UDF/PP composites

Fig. 5 presents the mechanical behavior induced by Iosipescu shear tests on UDF/PP composite at different fiber orientations. The three considered fiber orientations generate an elasto-plastic behavior. Specimens with θ = 90° show much higher strain than that of the other fiber orientations. Moreover, specimens with θ = 90° do not reach the fracture at the maximum displacement available with the Iosipescu testing system. Specimens with θ = 45° generate the highest stiffness, the lowest fracture strain and the lowest plastic zone.

This mechanical characterization proves that the fiber orientation affects strongly the shear behavior of UDF/PP composites and should be considered to investigate the cutting behavior because the mechanical stress in machining (dynamic mode) is apparent to the mechanical stress by an Iosipescu shear test (static mode) [15].

3.2. Chip morphology when cutting UDF/PP composites

Fig. 6 show the in-situ chip formation at different cutting conditions. The cutting speed has not a significant effect on the chip formation. The chip remains continuous at all the considered fiber orientations. However, changing the fiber orientation affects the chip curling. This cutting behavior regarding the fiber orientation is different from that of synthetic fiber composites as discussed in Section 1 where the fiber orientation in synthetic fiber composites controls the

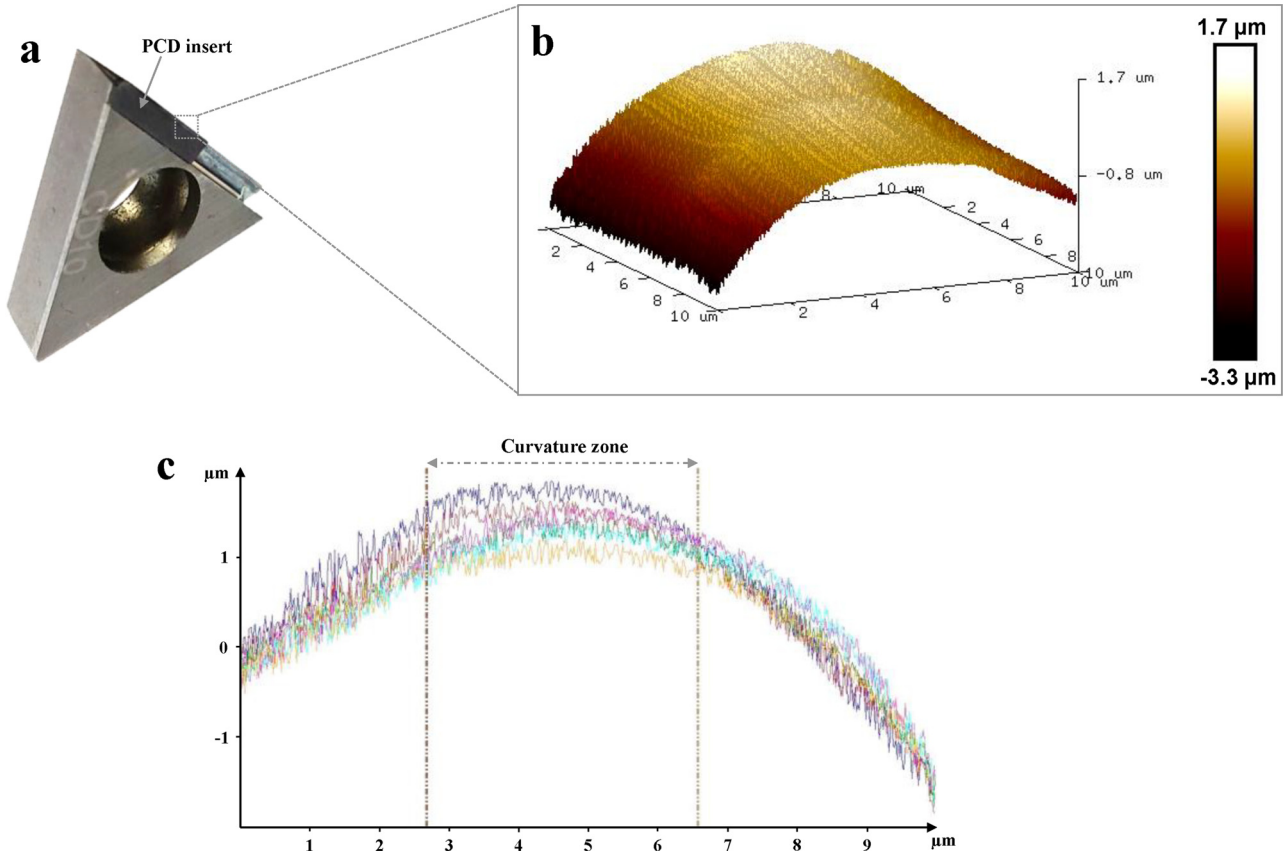

Fig. 4. a) PCD cutting insert. b) 3D surface topography of the cutting edge obtained by AFM. c) 2D profile sections of the cutting edge area taken at different locations.

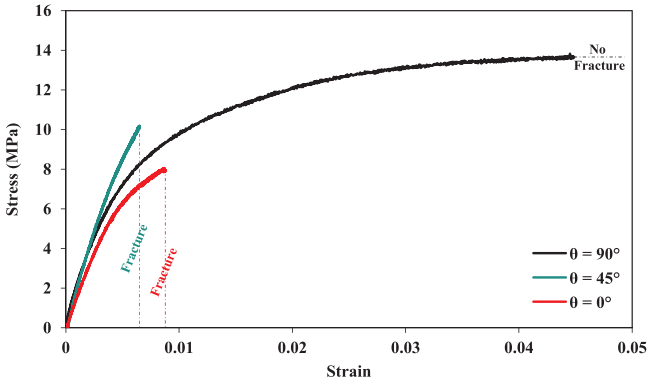

Fig. 5. Shear behavior curves of UDF/PP specimens for the considered fiber orientations.

interlaminar shearing and affects hence the formed chip (continuous, discontinuous, powder). For UDF/PP composites, the shear tests of Section 3.1 show an elasto-plastic behavior regardless of the fiber orientation which avoids brittle interlaminar fractures during the chip formation. At θ = 90°, flax fibers are perpendicular to the chip length direction and, therefore, the chip can deform and curl easily since there is less flexural resistance from fibers toward the chip length direction.

To calculate the chip thickness in function of the process parameters, the removed chips are embedded in epoxy resin perpendicularly to the width direction as shown in Fig. 7. The resulting worksurfaces are next polished with a fine grit size and then analyzed with SEM microscope. Fig. 7 shows SEM images of the removed chip sections. As for the chip formation, the SEM investigation does not reveal a significant effect of cutting speed on the chip sections. Therefore, only SEM images at the considered fiber orientation values are presented.

Since flax fibers are also oriented perpendicularly to the width direction, these latters are detached from the worksurface due to the polishing operation as shown in SEM images of Fig. 7. However, the resulting SEM images are useful to measure the mean chip thickness for each fiber orientation. The chip thickness is measured at ten locations on the chip section all over each SEM image in order to find a mean chip thickness for each configuration with a standard deviation. Therefore, the mean chip thickness is founded equal to $105^{\pm 5}$ µm for θ = 90°, $120^{\pm 7}$ µm for θ = 45° and $142^{\pm 10}$ µm for θ = 0°.

3.3. Machined surface characteristics at the microscale

Fig. 8 shows the microscopic state of flax fibers inside the composite material for the three considered fiber orientations after the cutting operations. The SEM images of Fig. 8 reveal the significant impact of fiber orientation on the cutting behavior of flax fibers. When flax fibers are oriented perpendicular to the cutting direction (θ = 90°), the fibers shearing is not efficient where uncut fibers extremities are observed on the machined surfaces (Fig. 8(a and d)). The fiber orientation $\theta = 45°$ shows the best flax fibers shearing since the fibers cross-sections can be observed in Fig. 8(b and e). On the other side, the cutting behavior of flax fibers oriented parallel to the cutting direction (θ = 0°) is random as it can be seen in Fig. 8(c and f). In this configuration, flax fibers are either sheared, detached, or torn-off inducing some defect zones. In general, and as for the chip study in Section 3.1, no significant cutting speed effect is observed from the SEM images.

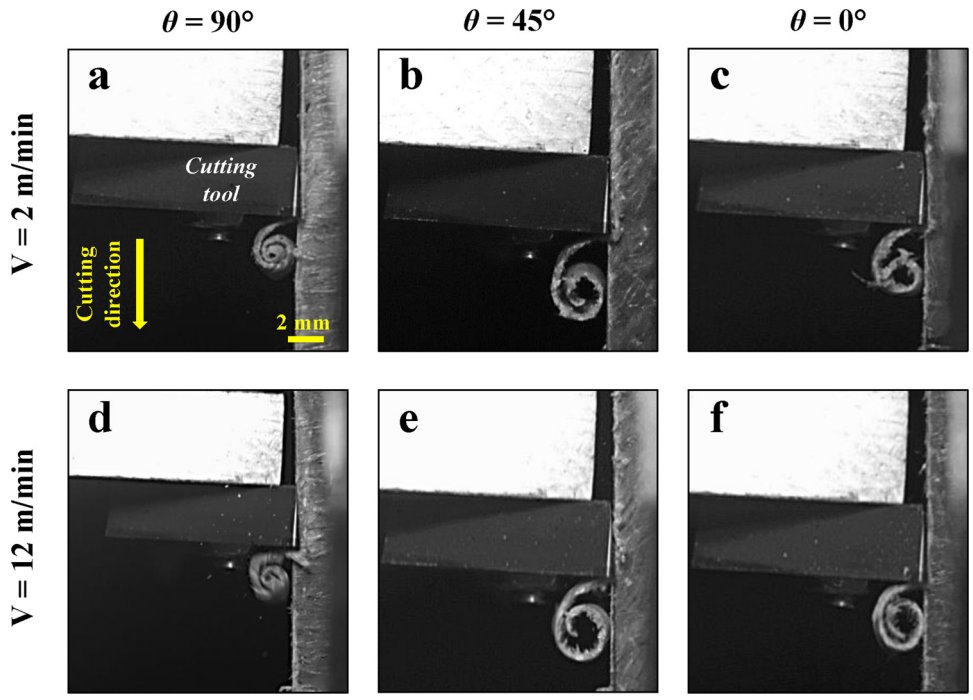

Fig. 6. Fast-cam images showing the in-situ chip morphology for different cutting conditions.

3.4. Application of Merchant model to the analysis of NFRP cutting behavior

3.4.1. Validity of Merchant model to NFRP machining

To apply Merchant model for synthetic fiber composites, the shear angle (ϕ) was substituted by the fiber orientation angle (θ) as explained in Section 1. This hypothesis cannot be considered for the cutting of NFRP composites because the removed chip remains continuous regardless of the fiber orientation value as shown in Section 3.2. The shear angle should be hence experimentally calculated using the chip thickness ratio.

The main assumptions that must be assumed for applying the Merchant model to NFRP cutting are as follows:

- The chip must remain continuous at all the cutting length (validated in Section 3.2);
- The chip does not flow to side and there is no side spread (validated in Section 3.2);
- The tool edge is sharp regarding the cutting depth (validated in Section 2.3);
- The chip width remains constant so the chip thickness ratio is equal to the chip length ratio.

The last assumption is validated in Table 2 by comparing the chip thickness ratio and the chip length ratio. The chip thickness ratio is calculated from the measurement of Section 3.2 as the ratio between the chip thickness and the cutting depth. The chip length ratio is

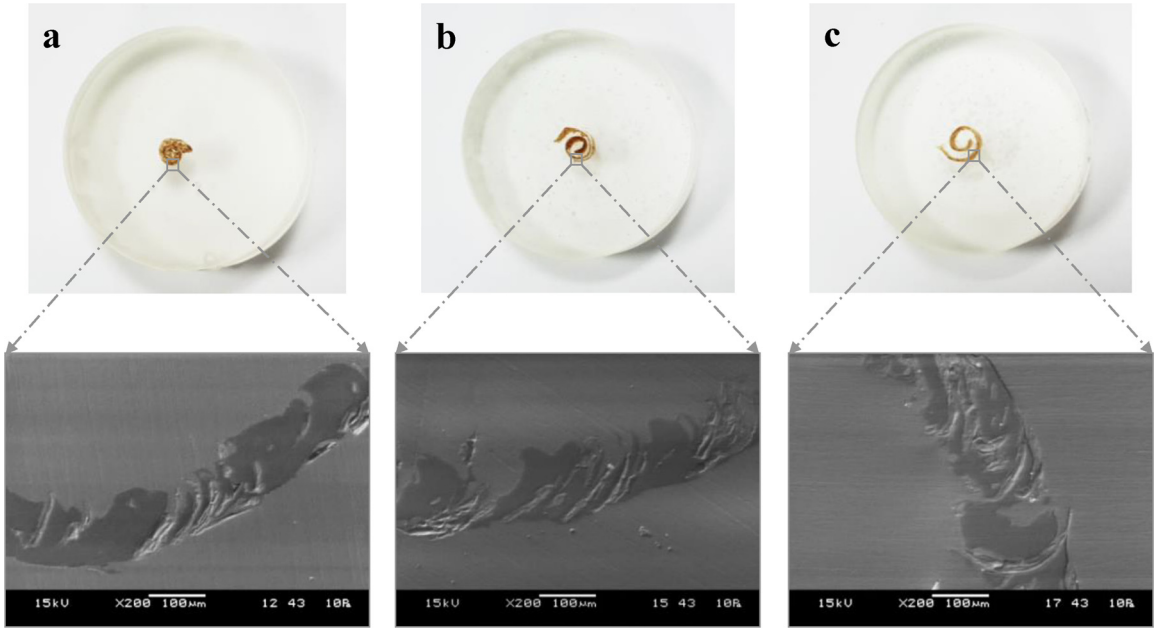

Fig. 7. SEM images of removed chip profile sections for the different fiber orientations: a) 90°, b) 45° and c) 0°.

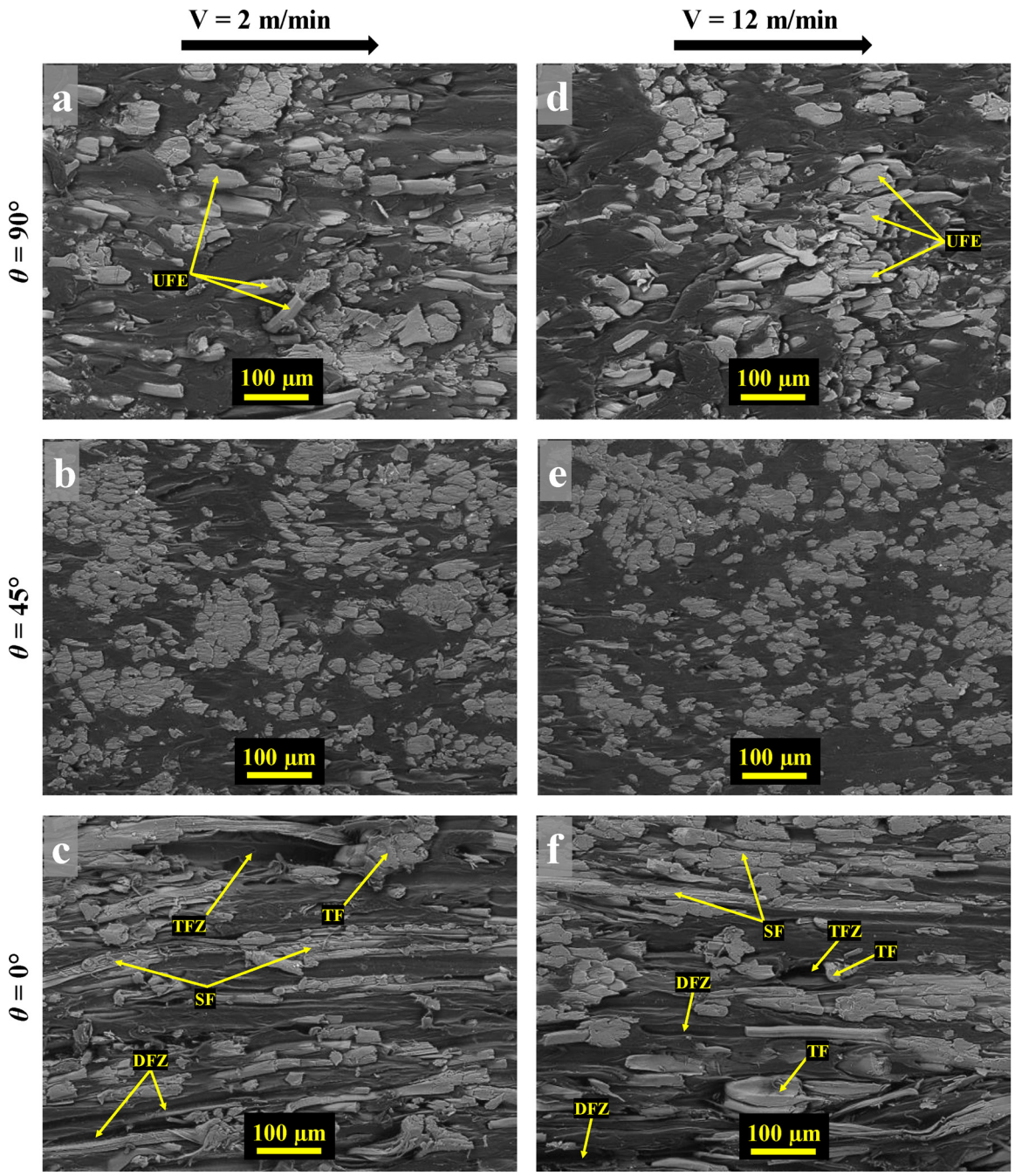

Fig. 8. SEM images showing the machined surfaces states of UDF/PP composites at different cutting conditions. "UFE": Uncut Fiber Extremities; "SF": Sheared Fibers; "TF": Torn-off Fibers; "TFZ": Torn-off Fibers Zone; "DFZ": Detached Fibers Zone.

Table 2
Comparison between chip thickness ratio and chip length ratio for the considered fiber orientations.

Fiber orientation	Chip length (µm)		Chip thickness (µm)		Chip thickness ratio				Chip length ratio			
	Min	Max	Min	Max	Min	Max	Mean	STD*	Min	Max	Mean	STD*
0°	13.5	14.5	132	152	0.76	0.66	**0.71**	**0.05**	0.68	0.73	**0.70**	**0.03**
45°	15.7	17.7	113	127	0.88	0.79	**0.84**	**0.05**	0.79	0.89	**0.84**	**0.05**
90°	17	19	100	110	1.00	0.91	**0.95**	**0.05**	0.85	0.95	**0.90**	**0.05**

* STD (standard deviation): the average of the absolute deviations of data values from their mean.

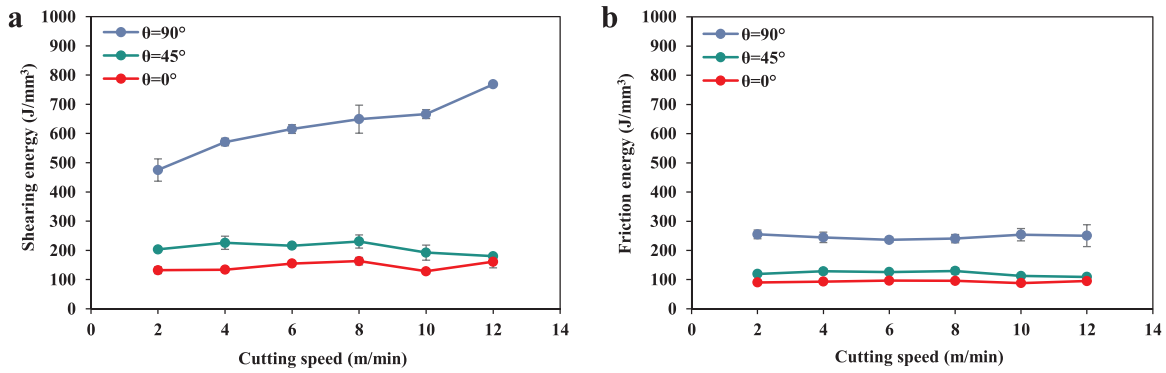

Fig. 9. Specific energies calculated using Merchant model during the cutting of UDF/PP composites for different fiber orientations. a) Specific shearing energy, and b) Specific friction energy.

calculated as the ratio between the removed chip length and the initial chip length. As for the chip thickness, cutting speed does not affect the removed chip length. However, reducing the fiber orientation from 90° to 0° reduces the removed chip length. The initial chip length before removal is equal to the sample length (20 mm) as mentioned in Section 2.3.

3.4.2. *Fiber orientation effect on the tribological cutting mechanisms*

Fig. 9 shows the evolution of both shearing and friction energies obtained by Merchant model [27]. Generally, cutting conditions with θ = 90° induce the highest energies while those with θ = 0° show the lowest energies. The cutting speed effect is insignificant except for the shearing energy with θ = 90° where increasing the cutting speed increases the shearing energy. It can also be noticed that the energy differences between θ = 45° and θ = 0° are slow comparing to the significant difference from the energies of cutting with θ = 90°, especially for the shearing energy (Fig. 9(a)).

The shearing energy behavior of Fig. 9(a) is compatible with the mechanical shear behavior of Fig. 5. Indeed, when flax fibers are oriented perpendicularly to the shear direction which is also the cutting direction (θ = 90°), UDF/PP samples are subjected to high strains due to the high transverse deformation of flax fibers. This makes the fiber shearing difficult and, then, increases considerably the shearing energy during the cutting operation. The shear strain of θ = 0° and θ = 45° is largely lower than that of θ = 90° as shown in Fig. 5 which can explain the significant difference in shearing energy between θ = 90° and the two other fiber orientations.

For more understanding of the cutting energies behavior, Fig. 10 illustrates the cutting contact between natural fibers and the cutting tool at the different considered fiber orientation. As explained in Section 1, natural fibers are themselves a composites material of cellulose microfibrils along with the fiber axis and natural amorphous polymers. Cellulose microfibrils have the major contribution to the fibers stiffness and, then, the fibers stiffness direction is also along with the fiber axis [25]. Therefore, the fiber orientation, which means the cellulose microfibrils orientation regarding the cutting direction, could have a significant impact on the cutting stiffness and, thus, the fibers cutting contact stiffness could be affected. When natural fibers are oriented with θ = 90°, cellulose microfibrils orientation is highly different from that of the shear force direction as illustrated in Fig. 10(b). Therefore, each elementary fiber will be transversely deformed until the cellulose microfibrils reach the shear force direction to get enough cutting contact stiffness. However, when natural fibers are oriented with θ = 45°, cellulose microfibrils orientation is in the shear force direction zone (Fig. 10(a)). The cutting contact stiffness in this case is then efficient for shearing fibers during cutting operation. Consequently, there is no significant fibers deformation before cutting.

On the other side, when natural fibers are oriented with θ = 0°, the fibers cutting behavior is random and depends on the cutting contact location (where the cutting edge radius is engaged at the beginning of the cutting contact) as previously demonstrated in [19] and shown in Fig. 11. Therefore, depending on the contact location and the high transverse elasticity of natural flax fibers, natural fibers are either sheared or plastically deformed from the cellulosic structure

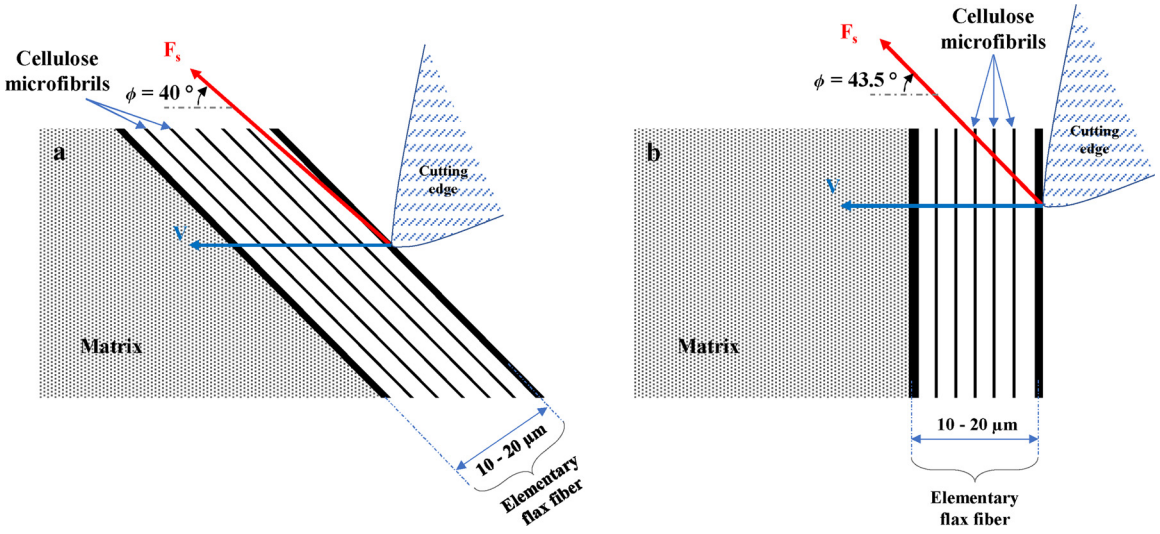

Fig. 10. Schematic illustration of the microscopic contact between the cutting tool edge and the flax fiber. a) at θ = 45° and b) at θ = 90°.

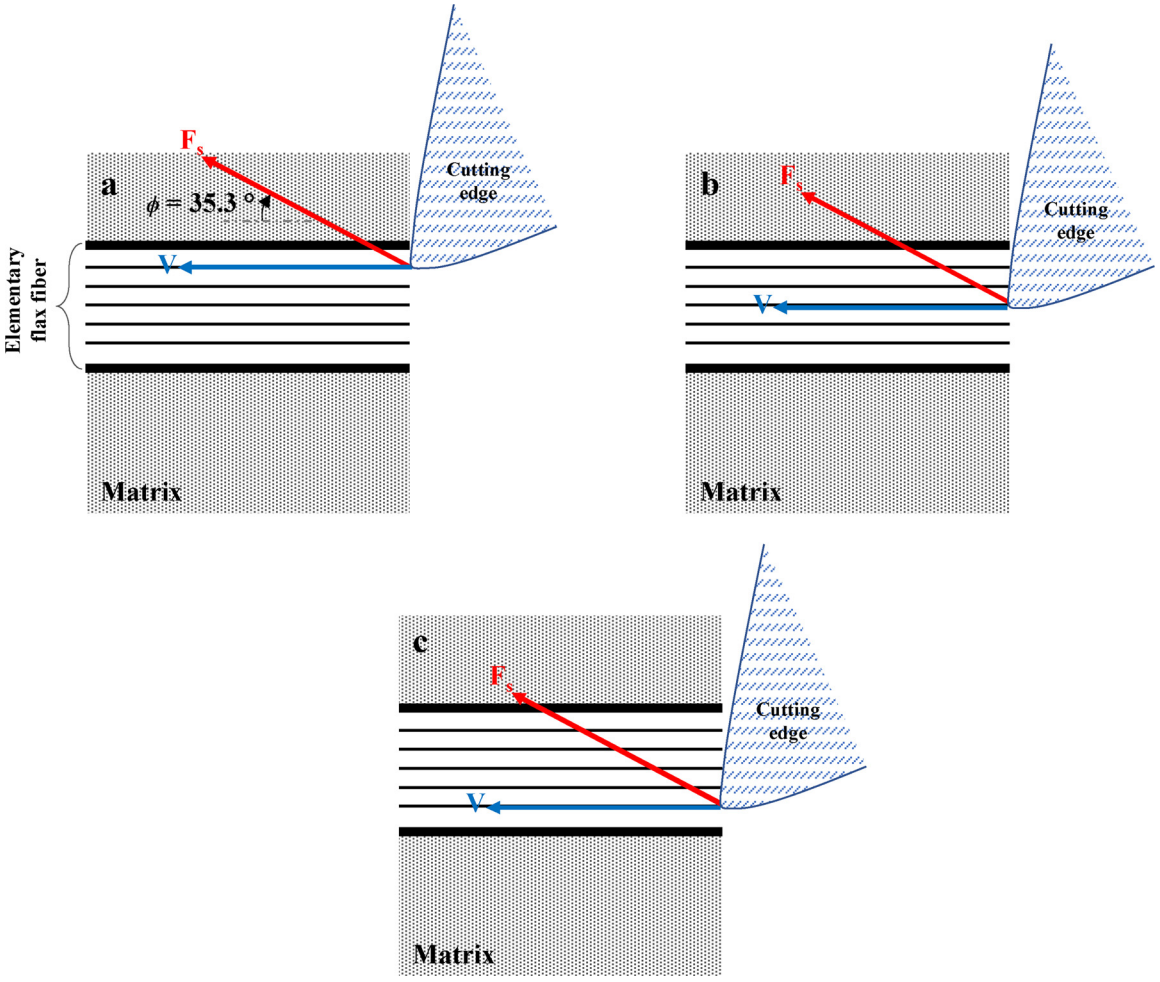

Fig. 11. Schematic illustration of the microscopic contact location between the cutting tool edge and the flax fiber when the fibers are oriented parallel to the cutting direction.

(Fig. 11(a)), torn-off by compressing the fiber (Fig. 11(b)), or detached by transverse flexion (Fig. 11(c)).

The friction energy is also related to the cutting behavior of flax fibers during the machining operation. Indeed, in the case of $\theta = 90°$, flax fibers are not efficiently sheared and incur a transverse deformation following the kinematics of the cutting tool. Therefore, in this cutting condition, there is an additional sliding contact component between flax fibers and the cutting tool edge before the fibers shearing which increases the energy dissipated by friction for $\theta = 90°$ as shown in Fig. 9(b). In contrast, when NFRP composite is machined with $\theta = 45°$, the fibers shearing is more efficient which reduces the additional sliding contact component and then decreases the friction energy. For $\theta = 0°$, the matrix is most concerned by the shearing mechanism during cutting. Thus, the additional sliding component between flax fibers and the cutting tool edge can be assumed negligible in this case which makes the friction energy the lowest for $\theta = 0°$.

3.5. Fiber orientation effect on machined surface roughness

The machinability analysis of NFRP composites requires the selection of the relevant scale that can discriminate the effect of material/process parameters on the machined surface topography [31]. This pertinent scale corresponds to the size of the natural fibrous structure inside the composites. For the considered UDF/PP composites, the fibrous structure is composed of flax fiber yarns that have cross-section diameters between 0.8 mm and 1 mm. The topographic resolution analysis in this study has been adapted to be in this scales range. Fig. 12 presents typical 3D topographic images of the machined surfaces obtained with an optical resolution of 840 × 840 μm. The optical interferometer can detect the cutting behavior of flax fibers at all the considered fiber orientations where the uncut fiber extremities, the sheared fibers, the torn-off fibers, and the detached fibers are captured.

To quantify these topographic measurements, Fig. 13 shows the arithmetic surface roughness evolution for the different cutting configurations. The fiber orientation is the most significant parameter that affects the surface roughness. As for the SEM observation of Fig. 8 and the energetic results of Fig. 9, the effect of the cutting speed is not significant comparing to the effect of the fiber orientation. Cutting with $\theta = 45°$ induces the lowest roughness while the orientation of 0° shows the highest roughness. Moreover, cutting the UDF/PP workpieces with $\theta = 0°$ induces high measurement deviations due the random cutting behavior shown in Fig. 8. Indeed, when flax fibers are not well sheared, both the uncut fiber extremities and the defect zones on the machined surface leads to an increase of the topographic irregularities which increases the surface roughness.

4. Conclusions

The present work aims to investigate the applicability of Merchant model to analyze the effect of fiber orientation on the machinability of NFRP composites with unidirectional flax fibers and polypropylene matrix (UDF/PP). The following conclusions can be drawn:

- Iosipescu shear tests show the significant effect of fiber orientation

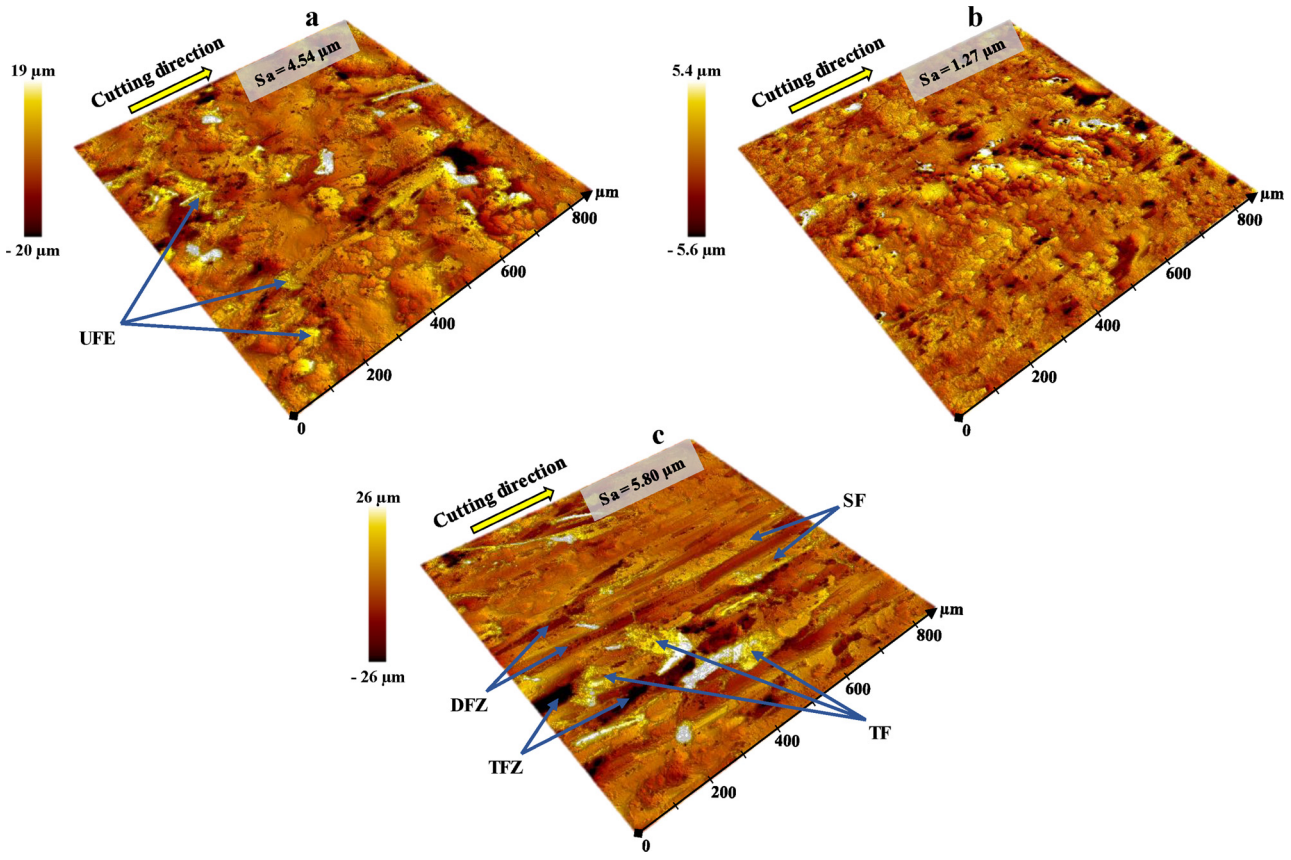

Fig. 12. Typical topographic images of UDF/PP machined surfaces at V = 8 m/min for different fiber orientations. a) θ = 90°, b) θ = 45° and c) θ = 0°. "UFE": Uncut Fiber Extremities; "SF": Sheared Fibers; "TF": Torn-off Fibers; "TFZ": Torn-off Fibers Zone; "DFZ": Detached Fibers Zone.

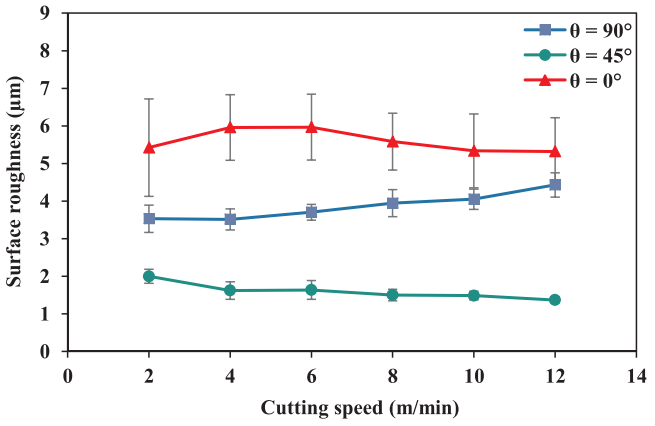

Fig. 13. Arithmetic surface roughness of UDF/PP machined surfaces at the different cutting conditions.

on the shear behavior of UDF/PP composites. When flax fibers are oriented perpendicularly to the shear direction (θ = 90°), UDF/PP composite generates a high ductile behavior with the highest shear strain while the configuration of θ = 45° provides the highest stiffness, the lowest shear strain and lowest plastic zone.

- The removed chip remains continuous regardless of the fiber orientation. However, the chip morphology is affected by the fiber orientation in terms of chip curling.
- Merchant model can be applied to investigate the tribological cutting mechanisms (shearing and friction) of UDF/PP composites. However, unlike synthetic fiber composites, the shear angle should not be assumed equal to the fiber orientation angle.
- The effect of fiber orientation is highly significant on the machined surfaces state. The fiber orientation $\theta = 45^{\circ}$ provides the best machinability with an efficient fibers shearing, the lowest surface roughness, in addition to low cutting energies dissipated by shearing and friction. This is related to the high shear stiffness involved by the fiber orientation of 45° as demonstrated by the mechanical shear tests.
- The orientation $\theta = 90^{\circ}$ generates the highest cutting energies because of the transverse deformation of flax fibers during the machining operation. However, the orientation $\theta = 0^{\circ}$ induces the highest surface roughness due to the random contact position between the cutting tool edge and flax fibers inside the composite.

References

[1] Shalwan A, Yousif BF. In State of Art: mechanical and tribological behaviour of polymeric composites based on natural fibres. Mater Des 2013;48:14–24. https://doi.org/10.1016/j.matdes.2012.07.014.
[2] Shah DU. Developing plant fibre composites for structural applications by optimising composite parameters: a critical review. J Mater Sci 2013;48:6083–107. https://doi.org/10.1007/s10853-013-7458-7.
[3] Bos HL, Müssig J, van den Oever MJA. Mechanical properties of short-flax-fibre reinforced compounds. Compos Part A Appl Sci Manuf 2006;37:1591–604. https://doi.org/10.1016/J.COMPOSITESA.2005.10.011.
[4] Goutianos S, Peijs T, Nystrom B, Skrifvars M. Development of flax fibre based textile reinforcements for composite applications. Appl Compos Mater 2006;13:199–215. https://doi.org/10.1007/s10443-006-9010-2.
[5] Jiang L, Walczyk D, McIntyre G, Bucinell R, Tudryn G. Manufacturing of biocomposite sandwich structures using mycelium-bound cores and preforms. J Manuf Process 2017;28:50–9. https://doi.org/10.1016/J.JMAPRO.2017.04.029.
[6] Ramesh M, Palanikumar K, Hemachandra Reddy K. Plant fibre based bio-composites: sustainable and renewable green materials. Renew. Sustain. Energy Rev 2017;79:558–84. https://doi.org/10.1016/J.RSER.2017.05.094.
[7] Yan L, Chouw N, Jayaraman K. Flax fibre and its composites – a review. Compos Part B Eng 2014;56:296–317. https://doi.org/10.1016/J.COMPOSITESB.2013.08.014.
[8] Mastura MT, Sapuan SM, Mansor MR, Nuraini AA. Materials selection of thermoplastic matrices for 'green' natural fibre composites for automotive anti-roll bar with

particular emphasis on the environment. Int J Precis Eng Manuf Technol 2018;5:111–9. https://doi.org/10.1007/s40684-018-0012-y.
[9] Ho M, Wang H, Lee J-H, Ho C, Lau K, Leng J, et al. Critical factors on manufacturing processes of natural fibre composites. Compos Part B Eng 2012;43:3549–62. https://doi.org/10.1016/J.COMPOSITESB.2011.10.001.
[10] Delahaigue J, Chatelain J-F, Lebrun G. Machining analysis of unidirectional and bi-directional flax-epoxy composite laminates. Proc Inst Mech Eng Part L J Mater Des Appl 2017;231:196–209. https://doi.org/10.1177/1464420716671970.
[11] Wang D, Onawumi PY, Ismail SO, Dhakal HN, Popov I, Silberschmidt VV, et al. Machinability of natural-fibre-reinforced polymer composites: conventional vs ultrasonically-assisted machining. Compos Part A Appl Sci Manuf 2019;119:188–95. https://doi.org/10.1016/J.COMPOSITESA.2019.01.028.
[12] Chegdani F, El Mansori M. Tribo-functional effects of double-crossed helix on surface finish, cutting friction and tool wear mechanisms during the milling process of natural fiber composites. Wear 2019;426–427:1507–14. https://doi.org/10.1016/J.WEAR.2018.11.026.
[13] Madhavan V, Lipczynski G, Lane B, Whitenton E. Fiber orientation angle effects in machining of unidirectional CFRP laminated composites. J Manuf Process 2015;20:431–42. https://doi.org/10.1016/J.JMAPRO.2014.06.001.
[14] Calzada KA, Kapoor SG, DeVor RE, Samuel J, Srivastava AK. Modeling and interpretation of fiber orientation-based failure mechanisms in machining of carbon fiber-reinforced polymer composites. J Manuf Process 2012;14:141–9. https://doi.org/10.1016/J.JMAPRO.2011.09.005.
[15] Bhatnagar N, Ramakrishnan N, Naik NK, Komanduri R. On the machining of fiber reinforced plastic (FRP) composite laminates. Int J Mach Tools Manuf 1995;35:701–16. https://doi.org/10.1016/0890-6955(95)93039-9.
[16] Nayak D, Bhatnagar N, Mahajan P. Machining studies of uni-directional glass fiber reinforced plastic (ud-gfrp) composites part 1: effect of geometrical and process parameters. Mach Sci Technol 2005;9:481–501. https://doi.org/10.1080/10910340500398167.
[17] Wang DH, Ramulu M, Arola D. Orthogonal cutting mechanisms of graphite/epoxy composite. Part I: unidirectional laminate. Int J Mach Tools Manuf 1995;35:1623–38. https://doi.org/10.1016/0890-6955(95)00014-O.
[18] Ramulu M, Wern CW, Garbini JL. Effect of fibre direction on surface roughness measurements of machined graphite/epoxy composite. Compos Manuf 1993;4:39–51. https://doi.org/10.1016/0956-7143(93)90015-Z.
[19] Chegdani F, Mezghani S, El Mansori M. On the multiscale tribological signatures of the tool helix angle in profile milling of woven flax fiber composites. Tribol Int 2016;100:132–40. https://doi.org/10.1016/j.triboint.2015.12.014.
[20] Nassar MMA Arunachalam R, Alzebdeh KI. Machinability of natural fiber reinforced composites: a review. Int J Adv Manuf Technol 2017;88:2985–3004. https://doi.org/10.1007/s00170-016-9010-9.
[21] Lotfi A, Li H, Dao DV, Prusty G. Natural fiber–reinforced composites: a review on material, manufacturing, and machinability. J Thermoplast Compos Mater 2019:089270571984454https://doi.org/10.1177/0892705719844546.
[22] Rajmohan T, Vinayagamoorthy R, Mohan K. Review on effect machining parameters on performance of natural fibre–reinforced composites (NFRCs). J Thermoplast Compos Mater 2019;32:1282–302. https://doi.org/10.1177/0892705718796541.
[23] Vinayagamoorthy R, Rajmohan T. Machining and its challenges on bio-fibre reinforced plastics: a critical review. J Reinf Plast Compos 2018;37:1037–50. https://doi.org/10.1177/0731684418778356.
[24] Roy Choudhury M, Srinivas MS, Debnath K. Experimental investigations on drilling of lignocellulosic fiber reinforced composite laminates. J Manuf Process 2018;34:51–61. https://doi.org/10.1016/J.JMAPRO.2018.05.032.
[25] Baley C. Analysis of the flax fibres tensile behaviour and analysis of the tensile stiffness increase. Compos - Part A Appl Sci Manuf 2002;33:939–48. https://doi.org/10.1016/S1359-835X(02)00040-4.
[26] Chegdani F, El Mansori M. Mechanics of material removal when cutting natural fiber reinforced thermoplastic composites. Polym Test 2018;67:275–83. https://doi.org/10.1016/j.polymertesting.2018.03.016.
[27] Merchant ME. Mechanics of the metal cutting process. I. Orthogonal cutting and a type 2 chip. J Appl Phys 1945;16:267. https://doi.org/10.1063/1.1707586.
[28] Silva LR, Davim JP, Abrão AM, Faria PE. Merchant model applied to precision orthogonal cutting of Pa66 polyamide with and without glass Fiber reinforcing. J Compos Mater 2009;43:2727–37. https://doi.org/10.1177/0021998309345312.
[29] Pierron F. Saint-venant effects in the Iosipescu Specimen. J Compos Mater 1998;32:1986–2015. https://doi.org/10.1177/002199839803202201.
[30] Ghidossi P, El Mansori M, Pierron F. Edge machining effects on the failure of polymer matrix composite coupons. Compos Part A Appl Sci Manuf 2004;35:989–99. https://doi.org/10.1016/j.compositesa.2004.01.015.
[31] Chegdani F, El Mansori M. New multiscale approach for machining analysis of natural fiber reinforced bio-composites. J Manuf Sci Eng 2018;141:11004. https://doi.org/10.1115/1.4041326.